Article ID: 1000-324X(2019)07-0786-05 **DOI:** 10.15541/jim20180455

Synthesis of Cubic-relievo Ag_3PO_4 with High Visible-light Photocatalytic Activity

WEI Ju-Meng, LÜ Qiang, WANG Ben-Chi, PAN Jia-Le, YE Xiang-Ju, SONG Chang-Chun

(College of Chemistry and Materials Engineering, Anhui Science and Technology University, Fengyang 233100, China)

Abstract: High visible-light photocatalytic activity silver phosphate (Ag_3PO_4) was successfully prepared *via* a facile water bath method. Scanning electron microscopy (SEM) images show that the products undergo three morphological changes during the reaction process, and the final product has uniform cubic-relievo morphology with an average particle size of about 1.6 μm. X-ray diffraction (XRD) patterns indicate that the samples are body-center cubic structure. In addition, the high resolution transmission electron microscopy (HRTEM) images show that several crystal facets are located in the surfaces of cubic-relievo Ag_3PO_4. UV-Vis absorption and photoluminescence (PL) spectra demonstrate that the products possess high visible-light responsive performance and weak PL emission intensity. The cubic-relievo Ag_3PO_4 exhibits significantly higher catalytic performance when applied on the photodegradation of methyl orange (MO) under visible-light irradiation in comparison to the cubic Ag_3PO_4, intermediate products or commercial nitrided TiO_2 photocatalyst. This work indicates that the photocatalytic performance of the catalyst can be effectively improved by changing its surface structure.

Key words: Ag_3PO_4; cubic-relievo; crystal faces; visible-light photocatalysis

Photocatalysis is an efficient technology for the degradation of organic contaminants[1]. In the past few decades, the search for photocatalysts is prevalent. To date, many wide band gap semiconductors, such as TiO_2, have been demonstrated to be excellent photocatalysts in the fields of photodegradation[2-3]. However, for those semiconductors with high band gap energy, only ultraviolet (UV) light (λ<400 nm), which is less than 4% of the solar spectrum can be effectively used in the process of photocatalytic reactions. Accordingly, the development of visible-light responsive photocatalysts is becoming increasingly important. Forming semiconductor heterojunction is an effective way to enhance the visible-light absorption[4]. Besides, exploring new type visible-light responsive photocatalysts has aroused growing research interest recently. Since 2010, Ag_3PO_4 with a band gap of 2.36 eV, as an emerging family of promising photocatalysts, has attracted much more attention[5-7]. To date, Ag_3PO_4 was confirmed as an excellent visible-light driven photocatalyst for water splitting and degradation of organic contaminants[8-11]. For instance, Ye's group[12] first demonstrated that Ag_3PO_4 had high visible-driven (λ>420 nm) water photooxidation, which could achieve a quantum efficiency as high as 90%. Yang, *et al*[13] reported that Ag_3PO_4 exhibited high photocatalytic activity for rhodamine B (RhB) degradation. Furthermore, in order to improve and optimize their photoelectric and photocatalytic properties, many methods have been developed. Among these methods, the morphology control has been considered to be one of the most promising avenues[14-15]. The morphology of materials is related to the exposed facets of the crystals, which directly affect the properties of the catalysts[16]. Therefore, adjusting the surface structures is a promising way to improve the photocatalytic activity of Ag_3PO_4.

In this work, a novel cubic-relievo shape Ag_3PO_4 with rugged surfaces was synthesized by a facile water bath method. The as-prepared final products showed high photocatalytic activity for the degradation of methyl orange (MO) under visible light irradiation.

1 Experimental

1.1 Reagent

Silver nitrate ($AgNO_3$, 99.9%), ammonium hydroxide ($NH_3\cdot H_2O$, 25%-28%), disodium hydrogen phosphate (Na_2HPO_4, 99%), alcohol (99.7%). All reagents were purchased from Sinopharm Chemical Reagent Co., Ltd,

Received date: 2018-09-26; **Modified date:** 2018-12-07

Foundation item: National Natural Science Foundation of China(21603002); Talent Introduction Foundation of Anhui Science and Technology University (ZRC2014448); Key Discipline Foundation of Anhui Science and Technology University (AKZDXK2015A01); The Open Foundation of Chongqing Key Laboratory of Environmental & Remediation Technologies (CEK1502); Foundation of College Students Innovation and Entrepreneurship (2017S10879012)

Biography: WEI Ju-Meng (1985–), PhD, lecturer. E-mail: weijm@ahstu.edu.cn

Corresponding author: SONG Chang-Chun, professor. E-mail: lzu_alice@163.com

and were used without further experimental purification.

1.2 Synthesis of Ag_3PO_4

The typical procedure includes three steps: (1) preparation of Tollens' reagents; (2) addition of Na_2HPO_4 solution; (3) reaction in water bath. Detailedly, 100 mg $AgNO_3$ was dissolved in 10 mL distilled water. Fresh Tollens' reagents was obtained when 30 mL, 0.1 mol/L ammonia solution was dropwise added to above $AgNO_3$ solution. Then, 20 mL, 0.15 mol/L Na_2HPO_4 aqueous solution was dropped into the above solution. Subsequently, the mixture was placed in a water bath at 30 ℃ for 24 h under magnetic stirring. It is noteworthy that Tollens' reagents and the reaction mixture should put into brown beaker flask in case photocorrosion occurs. Samples were extracted at schedule time (4, 12 and 24 h), corresponding to the initial, intermediate and final products, respectively. The obtained samples were washed with water and alcohol several times and dried in vacuum. The synthesis process and morphology evolution of samples are shown in Scheme 1.

1.3 Characterization

The structure of the samples were characterized by XRD (Rigaku D/Max-2400) using Cu-Kα radiation (40 kV, 60 mA, λ=0.1546 nm). The morphologies of the as-prepared Ag_3PO_4 were examined by field emission SEM, (TESCAN, MIRA3) and TEM (JEOL, JEM-2100F). UV-Visible absorption spectroscopy (ABs) was carried out by using a Shimadzu UV-3600 spectrophotometer. Photoluminescence (PL) spectrum was carried out on OmniPL-LF325 spectrofluorometer with 500 nm laser radiation source.

1.4 Photoreactivity measurements

In all of the photocatalytic activity experiments, the samples (10 mg) were made into an 100 mL aqueous MO solution to insure the equilibrium of the MO adsorption on the Ag_3PO_4. Then the solution was irradiated with a solution (5 mg/L) and stirred in the dark for 30 min to 500 W Xenon lamp with an ultraviolet cut-off filter (λ> 420 nm). During the irradiation, at given time intervals (10 min), 4 mL solution was sampled and centrifuged (10000 r/min) to remove the catalyst. The concentration of MB was calculated by measuring the absorbance of supernatants with a UV-3600 (Shimadzu) spectrophotometer.

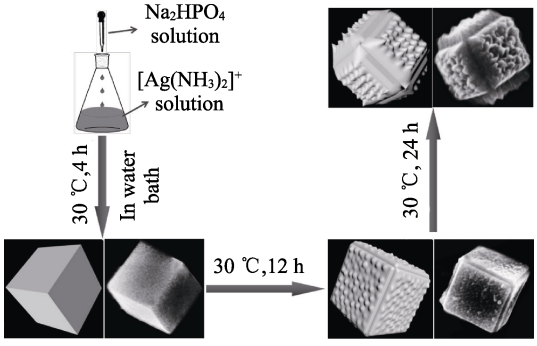

Scheme 1　Synthesis process and morphology evolution of Ag_3PO_4 with the reaction time extending

2 Results and discussion

As shown in Fig. 1(a)-(b), SEM images reveal that the initial products consist of uniform cubic microcrystals with average size of 1.6 μm. Figure 1(c) indicates that the average size of final products is still 1.6 μm, and the enlarged SEM image (Fig. 1(d)) reveals that the as-prepared final products are cubic-relievo shape with rugged surfaces. Based on these results, we propose that the cubic-relievo samples are generated from the cubic products through corrosion process. Furthermore, the morphology of intermediate products (Scheme 1) can also support this viewpoint. The cubic products were obtained within 4 h reaction. With the extension of reaction time, increasing amount of free $NH_3{\cdot}H_2O$ was released to the system (as reaction below).

$$HPO_4^{2-} \rightarrow PO_4^{3-} + H^+ \quad (1)$$

$$3\left[Ag\left(NH_3\right)_2\right]^+ + PO_4^{3-} + 6H_2O \rightarrow Ag_3PO_4^- + 6NH_3 \cdot H_2O \quad (2)$$

When the $NH_3{\cdot}H_2O$ concentration was high enough, the edges and the surfaces of the as-formed cubic products would be corroded by the free $NH_3{\cdot}H_2O$. As the corrosion process continues, the Ag_3PO_4 cubes would be corroded to form the final cubic-relievo shape with rugged surfaces. To the best of our knowledge, the cubic Ag_3PO_4 has been reported, yet this kind of novel morphology has been barely reported previously.

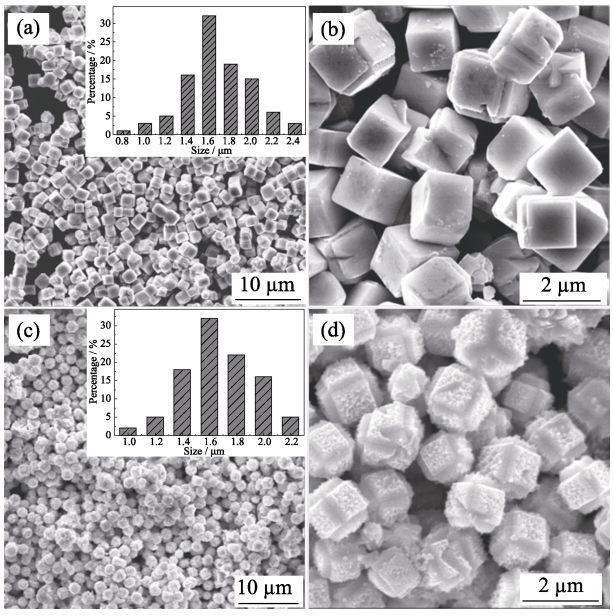

Fig. 1　Different magnification SEM images of initial (a-b), and final products(c-d) with insets showing the correponding histogram of size distribution

In order to investigate the structure of the as-obtained samples, the typical powder X-ray diffraction (XRD) was performed and the XRD patterns were shown in Fig. 2. The results indicate that the XRD patterns of both cubic and cubic-relievo samples can be well indexed to the body-centered cubic structure of Ag_3PO_4 (JCPDS 06-0505)[17]. The structure did not change with the different morphologies. The strong and sharp peaks suggest the highly crystalline nature of Ag_3PO_4 microcrystals. Figure 3 shows the high-resolution TEM (HRTEM) images of Ag_3PO_4 samples. As shown in Fig. 3(a), the lattice fringes of cubic-relievo Ag_3PO_4 have spacing of 0.30, 0.27, 0.24 and 0.19 nm, which is in agreement with the spacing of the (200), (210), (211) and (310) planes, respectively. It's worth noting that the (200), (211) and (310) planes locate in surfaces of cubic-relievo, and the Fig. 3(a) shows HRTEM images of (210) planes locating in the interior of the cubic-relievo Ag_3PO_4 crystal. For cubic Ag_3PO_4, by contrast, the lattice fringe spacing is 0.27 nm corresponding to (210) plane, which located in either surface or interior of the particles. The Fast Fourier Transform (FFT) patterns of HRTEM images are shown in the insets of Fig. 3(a)-(b). Two apparent rings (inset of Fig. 3(a)) indicate that several kinds of crystal facets exist in the surface of cubic-relievo Ag_3PO_4, and the distinct electron diffraction spots (inset of Fig.3(b)) show mono-crystalline nature of the cubic Ag_3PO_4 crystals. The FFT results are well corresponding to HRTEM images. However, the XRD pattern does not reveal any information about these crystal facets with different indexes, because these facets just exist in the subgrains below 2–5 nm surface (see the dashed circle in Fig. 3(a)) and account for tiny percentage of the Ag_3PO_4 particle. From this results, it can be inferred that corrosive effect of ammonia makes different crystal facets exposed to air.

The ultraviolet-visible diffuse reflectance spectra of cubic-relievo and cubic Ag_3PO_4 are shown in Fig. 4(a). The light absorption edges of the samples were achieved by extrapolating the steep slopes in the spectra. The cubic-relievo and cubic Ag_3PO_4 exhibits absorbance peak edges around 505 and 514 nm, respectively. Furthermore, for cubic-relievo Ag_3PO_4, the absorption intensity in the wavelength range from 380 nm to 500 nm is higher than that of cubic Ag_3PO_4. In our opinion, this enhancement is attributed to several crystal faces in the surfaces of cubic-relievo Ag_3PO_4. It's revealed that surface morphology is an important factor affecting diffusive reflectance spectra of the samples. The relationship between the coefficient and band gap energy can be described by the equation: $(\alpha h\nu)^2 = A(h\nu - E_g)$, in which α, ν, A, and E_g are absorption coefficient, light frequency, proportionality constant and band gap, respectively[18]. The plots of light energy $(\alpha h\nu)^2$ *versus* energy ($h\nu$) for the as-prepared samples are shown in Fig. 4(b), the band gap of cubic Ag_3PO_4 (2.47 eV) and cubic-relievo Ag_3PO_4 (2.45 eV) are evaluated by

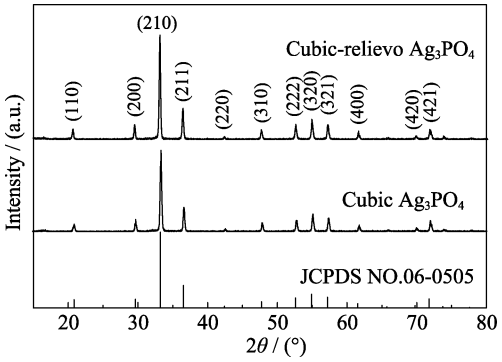

Fig. 2 XRD patterns of cubic and cubic-relievo products

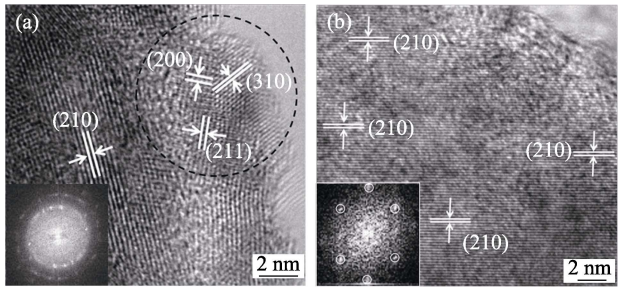

Fig. 3 HRTEM images of (a) cubic-relievo Ag_3PO_4 and (b) cubic Ag_3PO_4 with insets showing the correspongding FFT patterns of HRTEM images

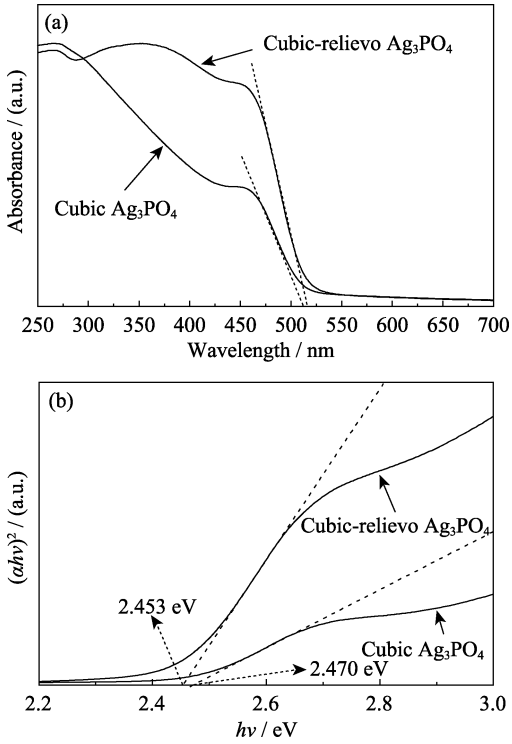

Fig. 4 (a) Ultraviolet-visible diffusive reflectance spectra, and (b) plots of light energy $(\alpha h\nu)^2$ *vs.* photon energy ($h\nu$) for the determination of the direct optical band gap of cubic-relievo Ag_3PO_4 and cubic Ag_3PO_4

extrapolating the straight line to the *hv* axis intercept. This slightly broadening of band gap is believed to have little effect on the photocatalytic activity.

The PL spectra of the as-prepared samples are performed to characterize the separation efficiency of the photo-generated electrons and holes[19]. As shown in Fig. 5, the cubic Ag_3PO_4 possess strong emission intensity in the range between 510–600 nm. Accordingly, this PL emission peaks usually generated from the recombination of electron and holes. However, the emission intensity of cubic-relievo Ag_3PO_4 is weaker than that of the cubic Ag_3PO_4. As it is well known, weaker PL intensity indicating higher separation efficiency, and which would lead to a higher photocatalytic activity[20]. It means that cubic-relievo Ag_3PO_4 should have higher efficiency for separating the photogenerated electron-holes.

As known to all, photocatalytic activity of materials depends not only on the crystal structure, but also on the surface structure[21]. Compared with cubic Ag_3PO_4, the novel cubic-relievo Ag_3PO_4 would present more crystal faces. In order to investigate the surface effects on the photocatalytic activity, the photocatalytic performance of cubic and cubic-relievo Ag_3PO_4 was evaluated by determining the degradation of MO under visible-light irradiation (λ>420 nm). For comparison, the performance of commercial nitrided TiO_2 and the intermediate product was also investigated, and the degradation efficiency is presented in Fig. 6(a). The adsorption abilities of the catalysts to MO are almost negligible in dark. Therefore, the photocatalytic activities are attributed to the degradation ability of the catalysts under visible-light irradiation. It is obvious that the cubic-relievo Ag_3PO_4 photocatalysts exhibited best photocatalytic activities for the MO degradation, and nearly 100% of MO was degraded after about 20 min irradiation under visible light irradiation. This results indicate that the photocatalytic activity of Ag_3PO_4 was significantly improved after the etching process with the extension of time. The cubic-relievo Ag_3PO_4 degraded 98% of MO and showed a photodegraded rate constant of 0.194 min^{-1}, representing a high photocatalytic activity (as shown in Fig. 6(b)).

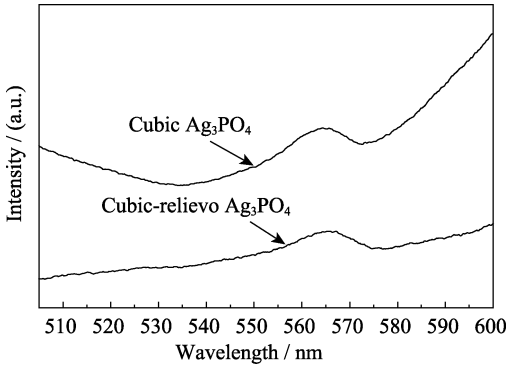

Fig. 5　PL emission spectra of cubic and cubic-relievo Ag_3PO_4

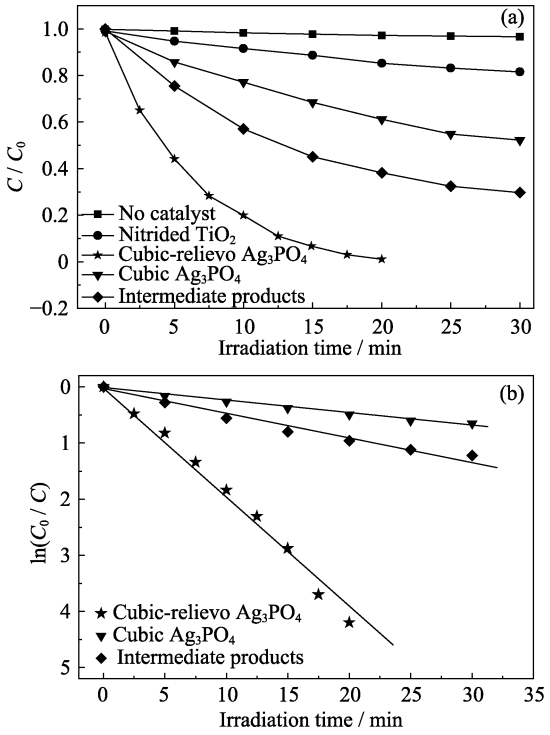

Fig. 6　Photocatalytic activities of MO over cubic-relievo Ag_3PO_4, cubic Ag_3PO_4 and commercial nitrided TiO_2 under visible- light irradiation (λ>420 nm) (a), the first-order rate constant of three types of Ag_3PO_4 on degradation of MO (b)

It is known that the photodegradation of organic pollutants is a surface oxidation process, which is driven by photogenerated electron-hole pairs correlated with the surface structure. For the photocatalytic behavior of Ag_3PO_4, the most crucial factor is the chemical adsorption and reaction of target molecules occurring on the surfaces of Ag_3PO_4. Therefore, The high photocatalytic activity of cubic-relievo Ag_3PO_4 can be attributed to the active sites exposed on the rugged surfaces. The schematic illustration of the catalytic mechanism is shown in Fig. 7. Several crystal facets exist in the rugged surfaces of cubic-relievo Ag_3PO_4, as we know, the photogenerated electrons on different crystal facets possess different energy and activity[16,21]. Moreover, the synergy between different crystal facets can enhance photocatalytic performance[22].

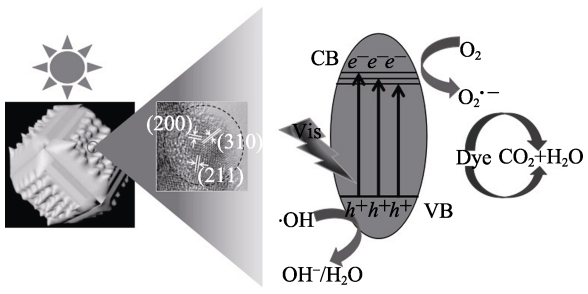

Fig. 7　Schematic illustration of the mechanism for the photocatalytic performance of cubic-relievo Ag_3PO_4

3 Conclusion

In conclusion, a novel cubic-relievo Ag_3PO_4 photocatalyst with rugged surfaces was prepared *via* a corrosion method. The evolution of the morphology form cubic to cubic-relievo shape has been investigated with the reaction time extending. The as-prepared cubic-relievo Ag_3PO_4 exhibited outstanding photocatalytic activity under visible-light irradiation. It is found that the different crystal facets exist on the surfaces of cubic-relievo Ag_3PO_4 which can effectively enhance the photocatalytic performance. This research proposed a new design and synthetic method to improve the performance by changing the surfaces of the materials.

References

[1] FUJISHIMA A, HONDA K. Electrochemical photolysis of water at a semiconductor electrode. *Nature*, 1972, **238:** 37–38.

[2] LIU B, HUANG Y, WEN Y, *et al*. Highly dispersive {001} facets-exposed nanocrystalline TiO_2 on high quality graphene as a high performance photocatalyst. *J. Mater. Chem*., 2012, **15(22):** 7484–7491.

[3] KSIBI M, ROSSIGNOL S, TATIBOUET J M, *et al*. Synthesis and solid characterization of nitrogen and sulfur-doped TiO_2 photocatalysts active under near visible light. *Mater. Lett*., 2008, **62(26):** 4204–4206.

[4] HUANG S, XU Y, ZHOU T, *et al*. Constructing magnetic catalysts with *in-situ* solid-liquid interfacial photo-Fenton-like reaction over Ag_3PO_4@$NiFe_2O_4$ composites. *Appl. Catal. B: Environ.*, 2018, **225:** 40–50.

[5] BI Y, OUYANG S, CAO J, *et al*. Facile synthesis of rhombic dodecahedral AgX/Ag_3PO_4 (X = Cl, Br, I) heterocrystals with enhanced photocatalytic properties and stabilities. *Phys. Chem. Chem. Phys*., 2011, **13(21):** 10071–10075.

[6] JIAO Z, ZHANG Y, YU H, *et al*. Concave trisoctahedral Ag_3PO_4 microcrystals with high-index facets and enhanced photocatalytic properties. *Chem. Commun*., 2013, **49(6):** 636–638.

[7] DONG P, WANG Y, LI H, *et al*. Shape-controllable synthesis and morphology-dependent photocatalytic properties of Ag_3PO_4 crystals. *J. Mater. Chem. A*, 2013, **1(15):** 4651–4656.

[8] MARTIN D J, UMEZAWA N, CHEN X, *et al*. Facet engineered Ag_3PO_4 for efficient water photooxidation. *Energy Environ. Sci.*, 2013, **6(11):** 3380–3386.

[9] ZHAI W, LI G, YU P, *et al*. Silver phosphate/carbon nanotube-stabilized pickering emulsion for highly efficient photocatalysis. *J. Phys. Chem. C*, 2013, **117(29):** 15183–15191.

[10] DINH C T, NGUYEN T D, KLEITZ F, *et al*. Large-scale synthesis of uniform silver orthophosphate colloidal nanocrystals exhibiting high visible light photocatalytic activity. *Chem. Commun.*, 2011, **47(27):** 7797–7799.

[11] BI Y, HU H, OUYANG S, *et al*. Selective growth of Ag_3PO_4 submicro-cubes on Ag nanowires to fabricate necklace-like heterostructures for photocatalytic applications. *J. Mater. Chem.*, 2012, **22(30):** 14847–14850.

[12] YI Z, YE J, KIKUGAWA N, *et al*. An orthophosphate semiconductor with photooxidation properties under visible-light irradiation. *Nature Mater*., 2010, **9(7):** 559–564.

[13] LIANG Q, MA W, SHI Y, *et al*. Hierarchical Ag_3PO_4 porous microcubes with enhanced photocatalytic properties synthesized with the assistance of trisodium citrate. *CrystEngComm*, 2012, **14(8):** 2966–2973.

[14] GUO X, CHEN C, YIN S, *et al*. Controlled synthesis and photocatalytic properties of Ag_3PO_4 microcrystals. *J. Alloy. Comp*., 2015, **619:** 293–297.

[15] WANG J, TENG F, CHEN M, *et al*. Facile synthesis of novel Ag_3PO_4 tetrapods and the {110} facets-dominated photocatalytic activity. *CrystEngComm*, 2013, **15(1):** 39–42.

[16] BI Y, OUYANG S, UMEZAWA N, *et al*. Facet effect of single-crystalline Ag_3PO_4 sub-microcrystals on photocatalytic properties. *J. Am. Chem. Soc*., 2011, **133(17):** 6490–6492.

[17] MARTIN D J, LIU G, MONIZ S J A, *et al*. Efficient visible driven photocatalyst, silver phosphate: performance, understanding and perspective. *Chem. Soc. Rev*., 2015, **46(50):** 7808–7828.

[18] BUTLER M A. Photoelectrolysis and physical properties of the semiconducting electrode WO_2. *J. Appl. Phys*., 1977, **48(5):** 1914–1920.

[19] CHENG J, YAN X, MO Q, *et al.* Facile synthesis of g-C_3N_4/$BiVO_4$ heterojunctions with enhanced visible light photocatalytic performance. *Ceram. Internat*., 2017, **43(1):** 301–307.

[20] CHEN L, YU Y, WU M, *et al.* Synthesis of hollow $BiVO_4$/Ag composite microspheres and their photocatalytic and surface enhanced raman scattering propertiesl. *ChemPlusChem*, 2015, **80(5):** 871–877.

[21] ZHENG B, WANG X, LIU C, *et al*. High-efficiently visible light-responsive photocatalysts**:** Ag_3PO_4 tetrahedral microcrystals with exposed {111} facets of high surface energy. *J. Mater. Chem. A*, 2013, **1(40):** 12635–12640.

[22] CAO M, TANG Z, LIU Q, *et al*. The Synergy between metal facet and oxide support facet for enhanced catalytic performance: the case of Pd-TiO_2. *Nano Lett*., 2016, **16(8):** 5298–5302.

高可见光催化活性立方体浮雕状 Ag_3PO_4 的合成

魏居孟, 吕 强, 王奔驰, 潘家乐, 叶祥桔, 宋常春

(安徽科技学院 化学与材料工程学院, 凤阳 233100)

摘 要: 采用简单的水浴法成功制备了具有高可见光活性的 Ag_3PO_4 材料。扫描电镜测试结果表明反应过程中产物经历了三种形貌的演变, 最终产物具有均一的立方体浮雕形貌, 平均颗粒尺寸大小约为 1.6 μm。通过 X 射线衍射图谱可知产物具有体心立方结构。此外, 从高倍透射电镜图片中可判断出样品表面存在多种晶面。紫外–可见吸收光谱和荧光光谱结果表明该产物具有高的响应可见光的性能和较弱的荧光发射强度。该产物与立方 Ag_3PO_4、反应的中间产物和商用氮化的 TiO_2 催化剂相比, 在可见光下对甲基橙的降解表现出有显著的催化活性。研究工作表明, 通过改变催化剂的表面结构可以有效提高材料的光催化性能。

关 键 词: 磷酸银; 立体浮雕状; 多种晶面; 可见光催化

中图分类号: TQ174 **文献标识码:** A